

Supplementary Materials: Antarctic Ice Mass Change Products from GRACE/GRACE-FO using Tailored Sensitivity Kernels

Andreas Groh ^{1,*}  and Martin Horwath ¹ 

1. Tailored Sensitivity Kernels

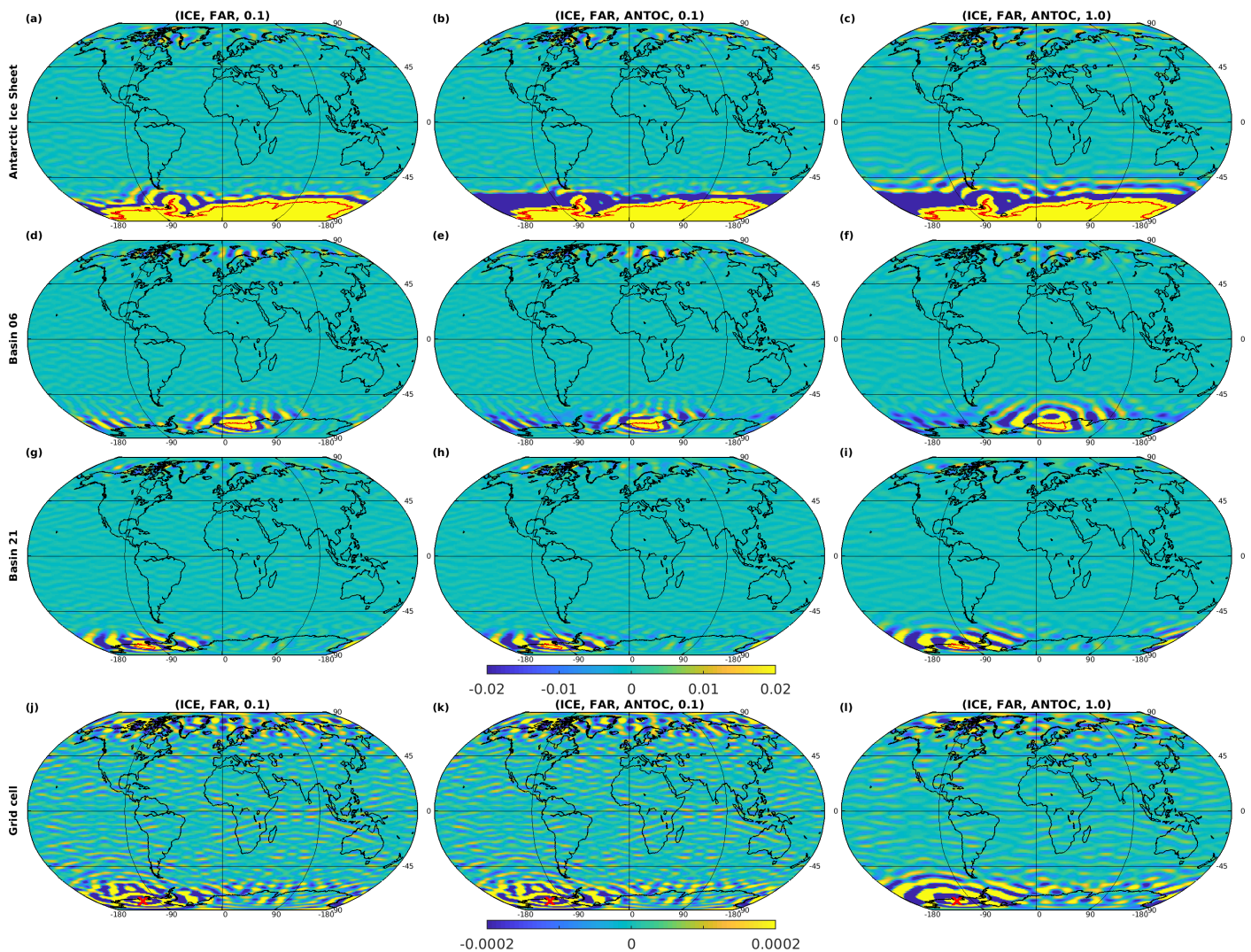


Figure S1. Global view on different realisations (columns) of tailored sensitivity kernels for integrating mass changes of the Antarctic Ice Sheet, Basin 06, Basin 21 and a single grid cell (rows). Red lines depict the basin outlines. Please note the differing colour scales for panels (a)–(i) and (j)–(l). All colour bars are truncated to provide a more detailed view on variations around zero.

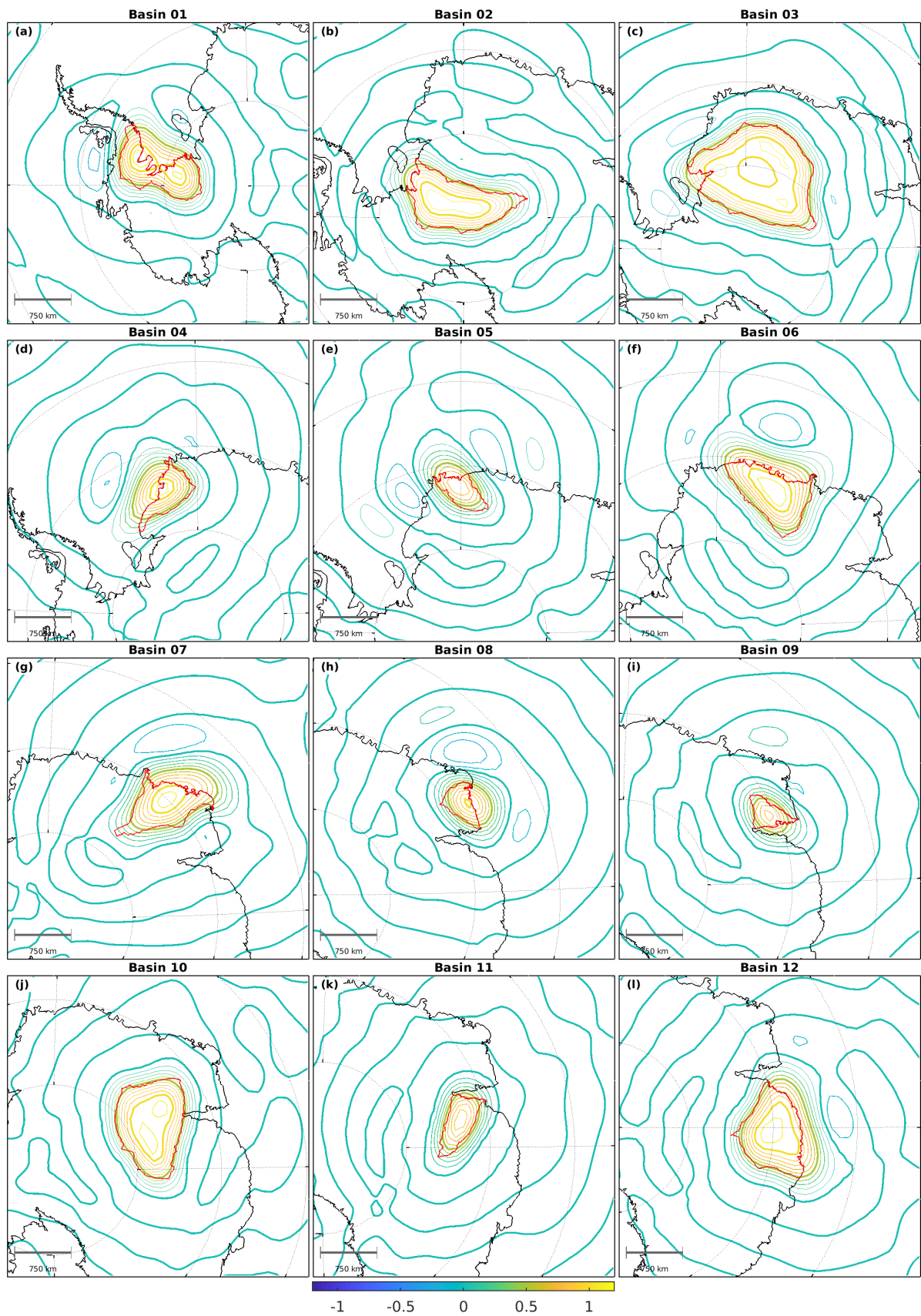


Figure S2. Variant (ICE,FAR,ANTOC,1.0) of the tailored sensitivity kernels for (a)–(l) Basin 01 – Basin 12. Contour lines (thin) are given at intervals of 0.1, thick contours lines are shown for multiples of 0.5. Red lines depict the basin outlines.

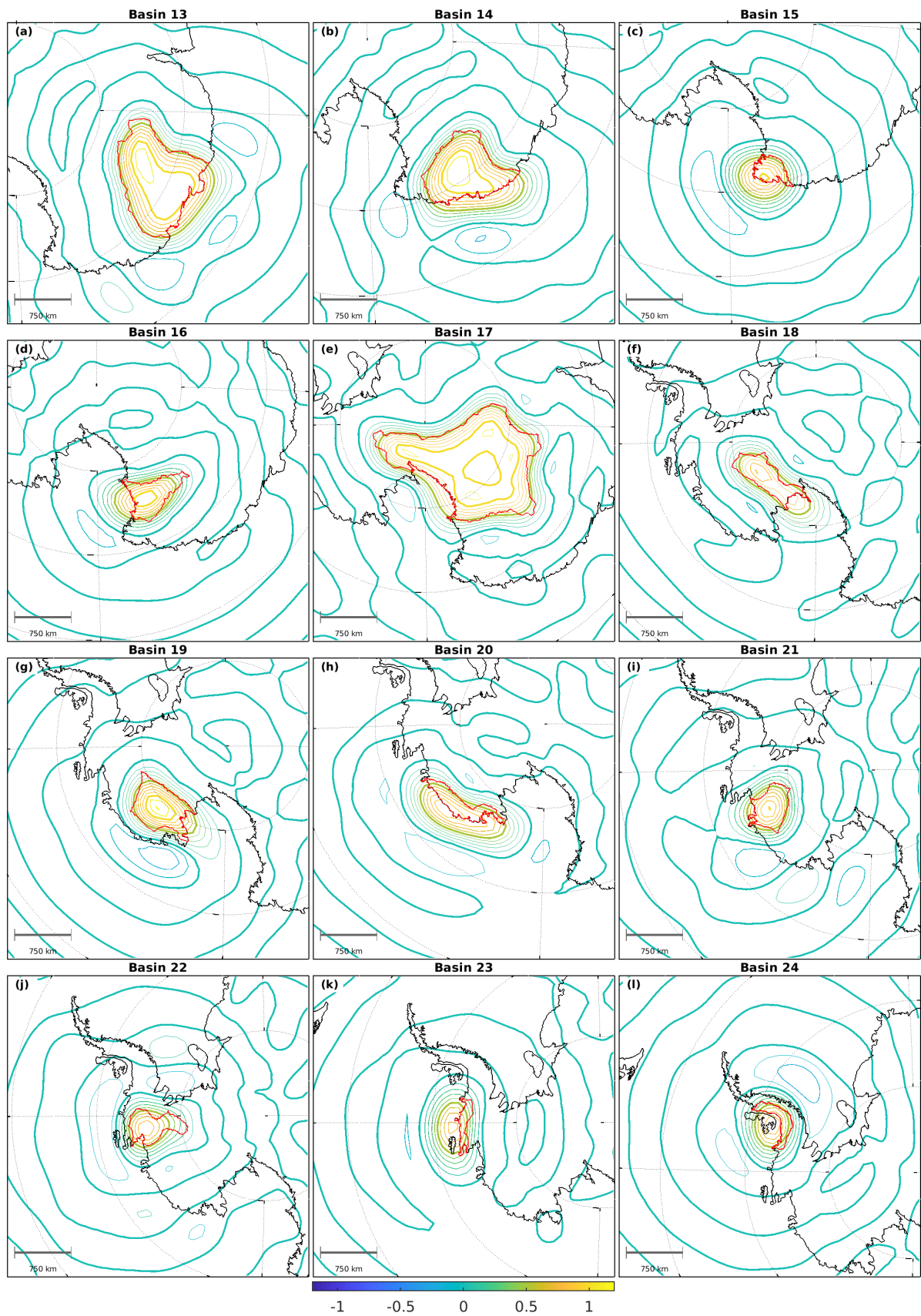


Figure S3. Variant (ICE,FAR,ANTOC,1.0) of the tailored sensitivity kernels for (a)–(l) Basin 13 – Basin 24. Contour lines (thin) are given at intervals of 0.1, thick contours lines are shown for multiples of 0.5. Red lines depict the basin outlines.

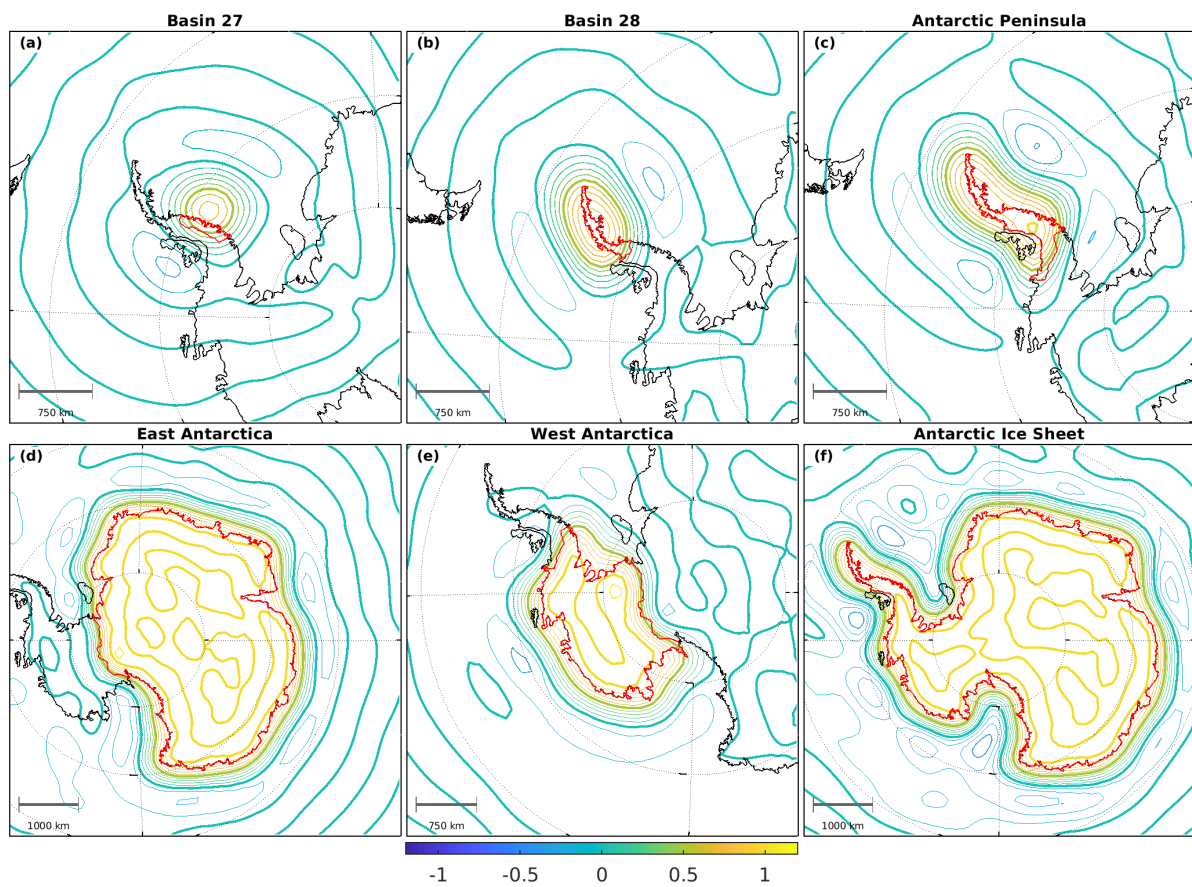


Figure S4. Variant (ICE,FAR,ANTOC,1.0) of the tailored sensitivity kernels for (a)–(b) Basin 27 – Basin 28, (c) the Antarctic Peninsula, (d) East Antarctica, (e) West Antarctica and (f) the Antarctic Ice Sheet. Contour lines (thin) are given at intervals of 0.1, thick contours lines are shown for multiples of 0.5. Red lines depict the basin outlines.

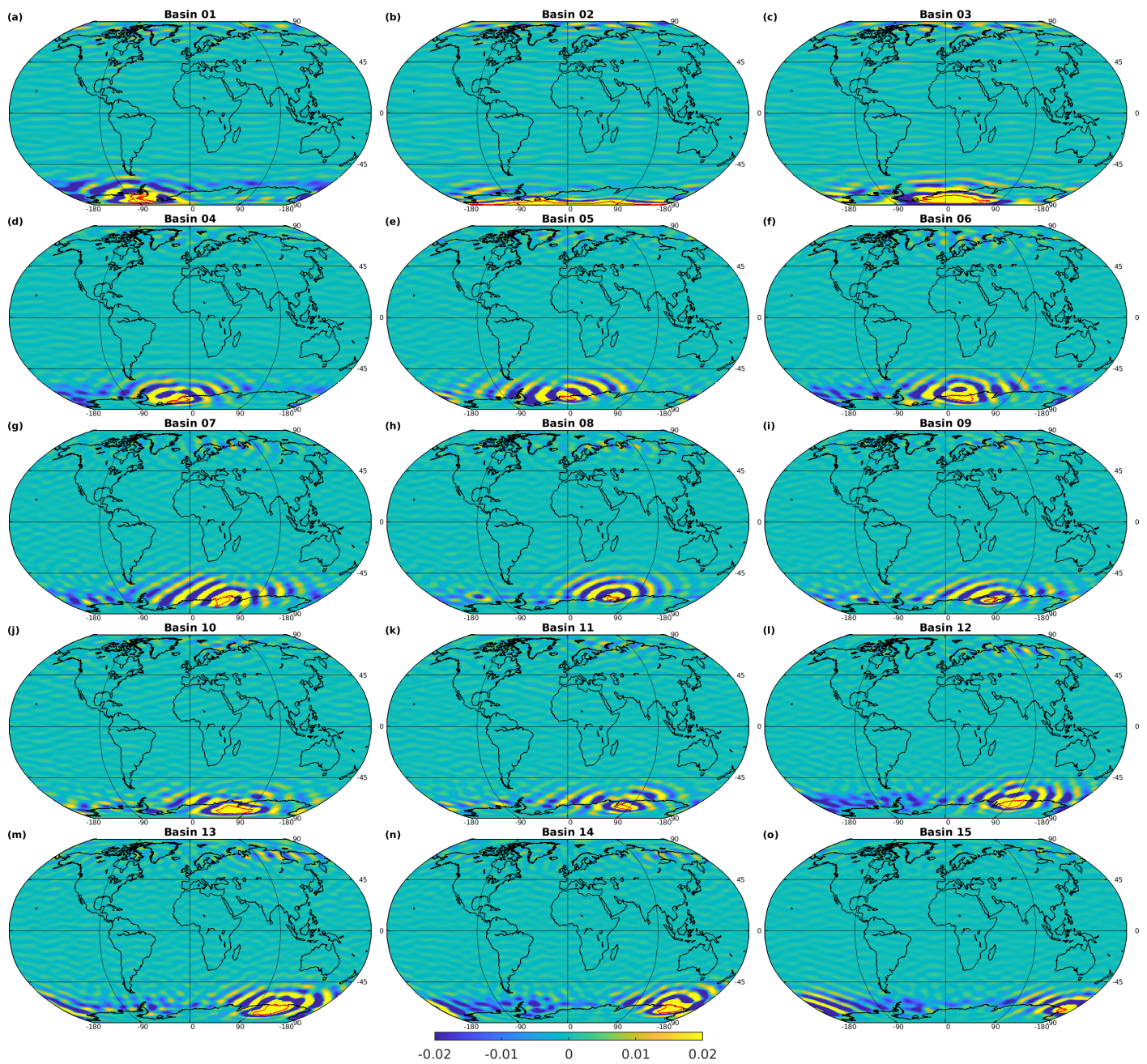


Figure S5. Global view on the (ICE,FAR,ANTOC,1.0)-variant of the tailored sensitivity kernels for (a)–(o) Basin 01 – Basin 15. Red lines depict the basin outlines. All colour bars are truncated to provide a more detailed view on variations around zero.

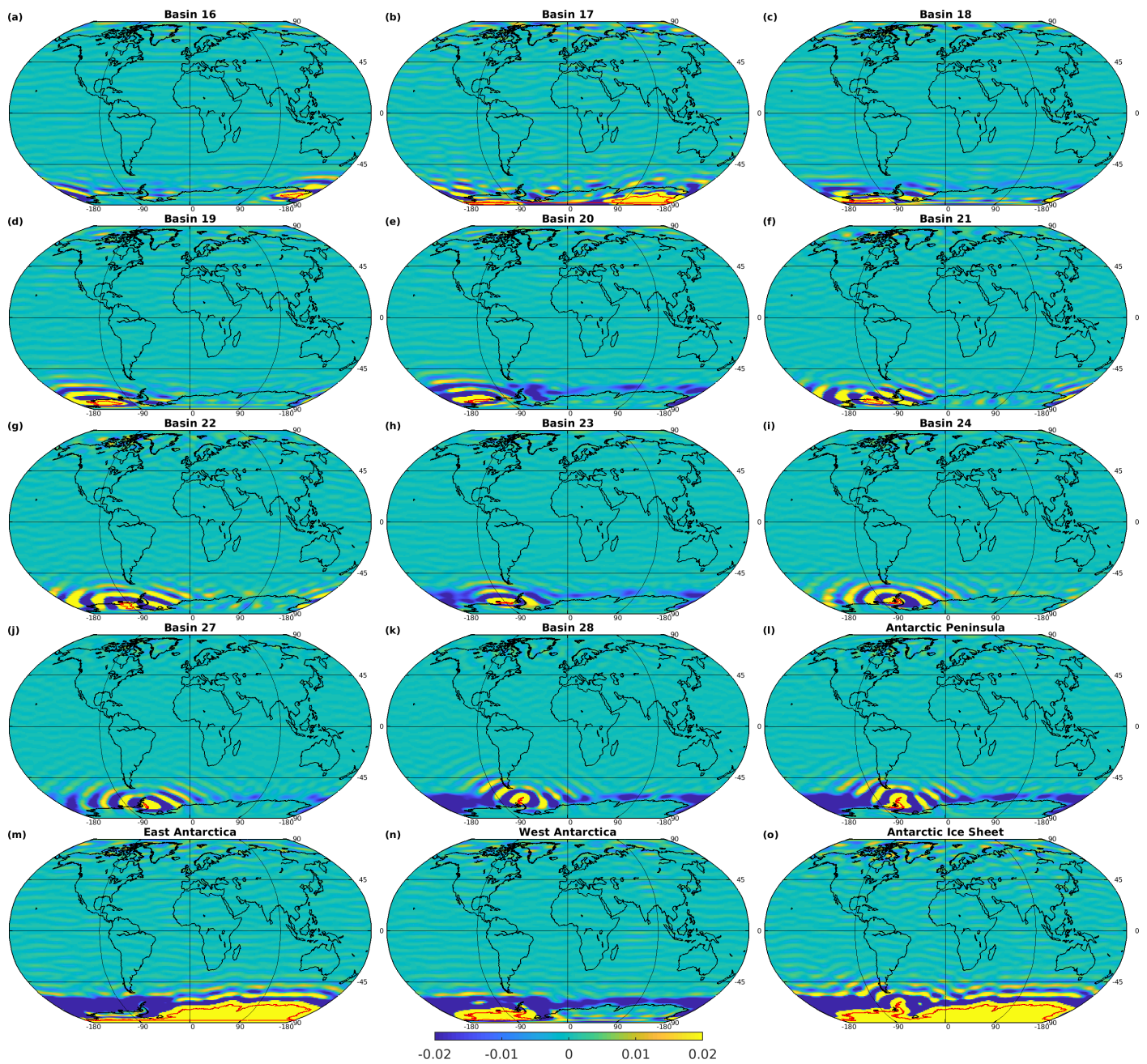


Figure S6. Global view on the (ICE,FAR,ANTOC,1.0)-variant of the tailored sensitivity kernels for (a)–(k) Basin 06 – Basin 28, (l) the Antarctic Peninsula, (m) East Antarctica, (n) West Antarctica and (o) the Antarctic Ice Sheet. Red lines depict the basin outlines. All colour bars are truncated to provide a more detailed view on variations around zero.

2. Mass Change Time Series

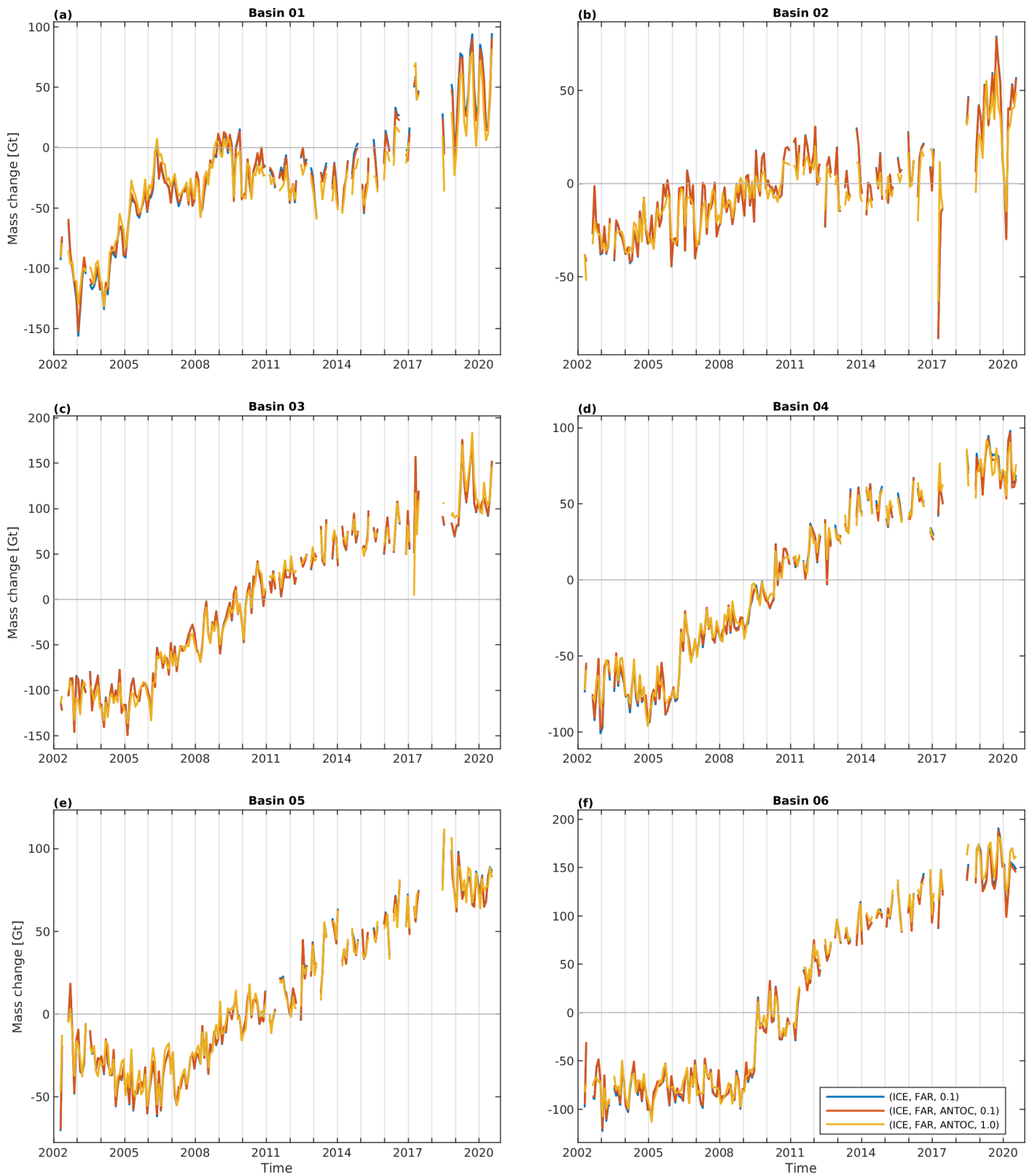


Figure S7. (a)–(f) Mass change time series for Basin 01 – Basin 06 derived using different realisations of tailored sensitivity kernels.

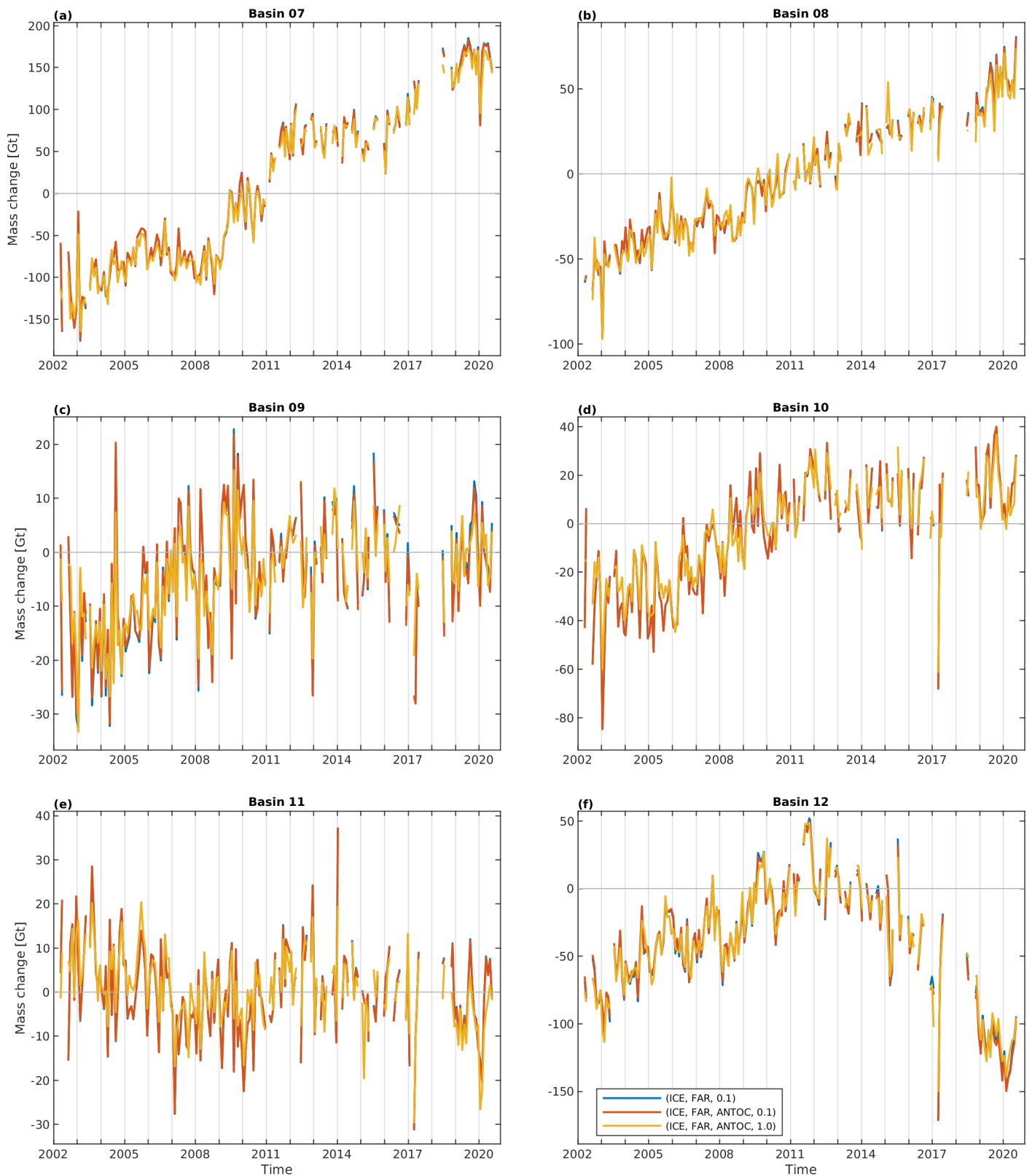


Figure S8. (a)–(f) Mass change time series for Basin 07 – Basin 12 derived using different realisations of tailored sensitivity kernels.

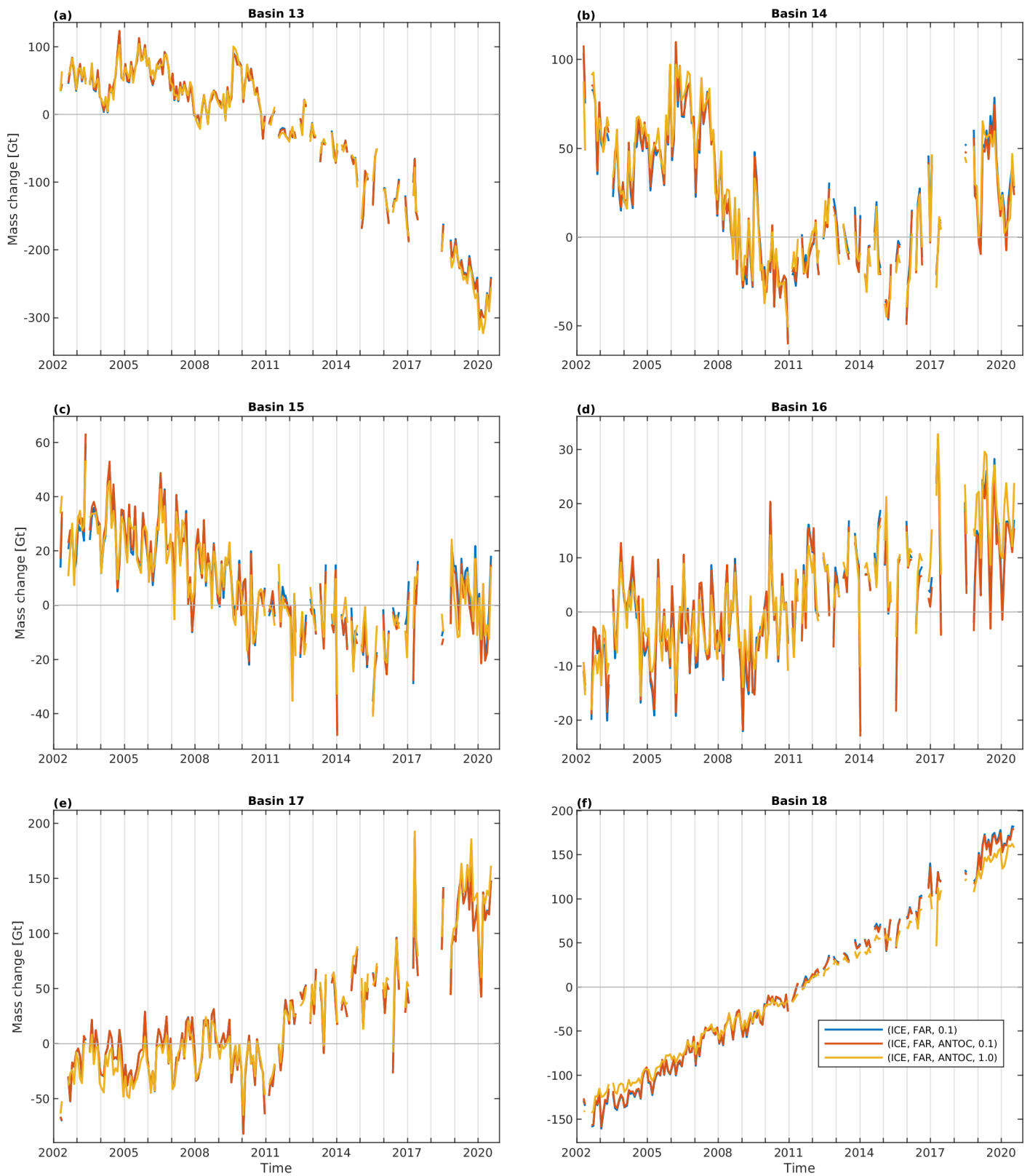


Figure S9. (a)–(f) Mass change time series for Basin 13 – Basin 18 derived using different realisations of tailored sensitivity kernels.

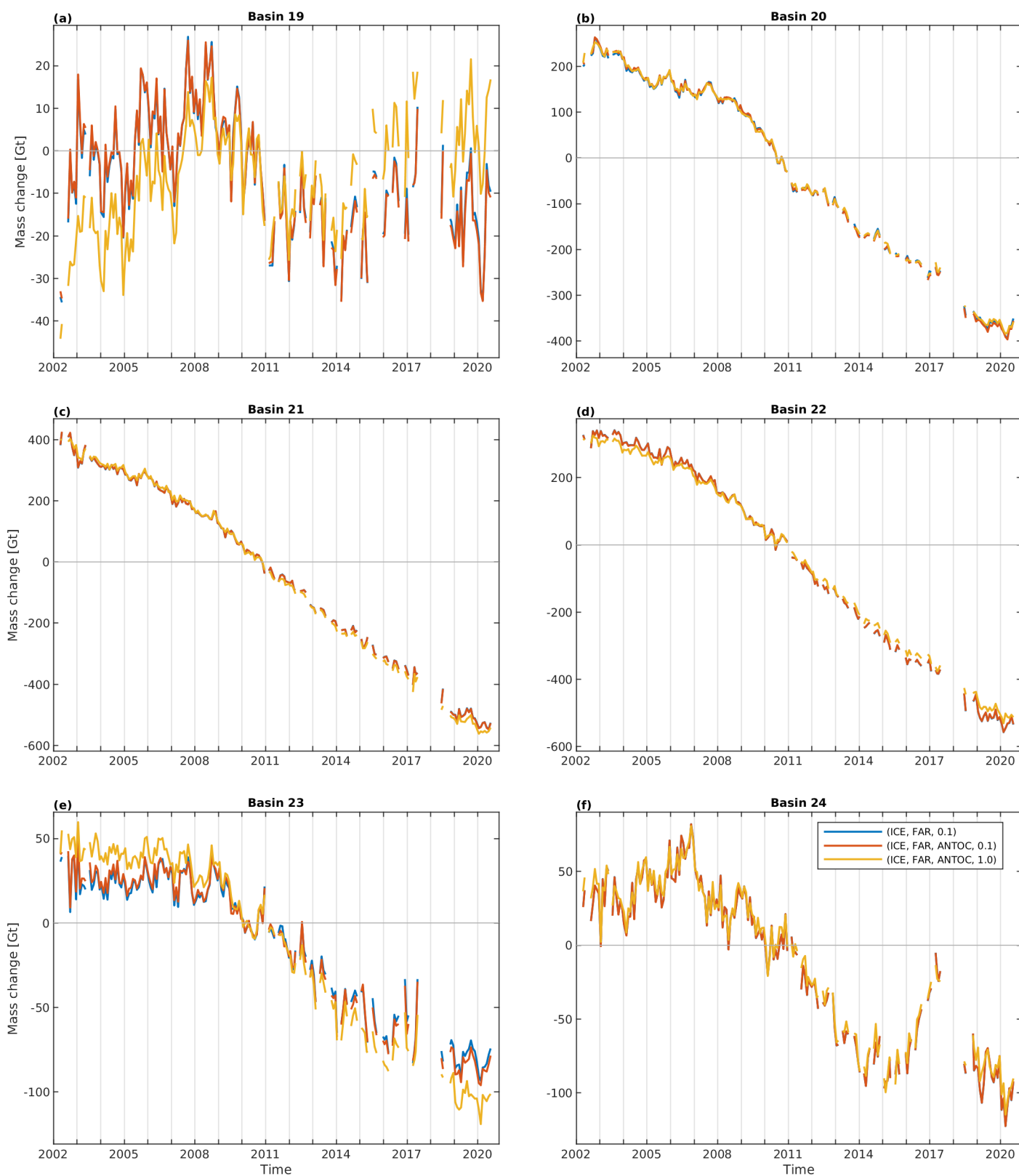


Figure S10. (a)–(f) Mass change time series for Basin 19 – Basin 24 derived using different realisations of tailored sensitivity kernels.

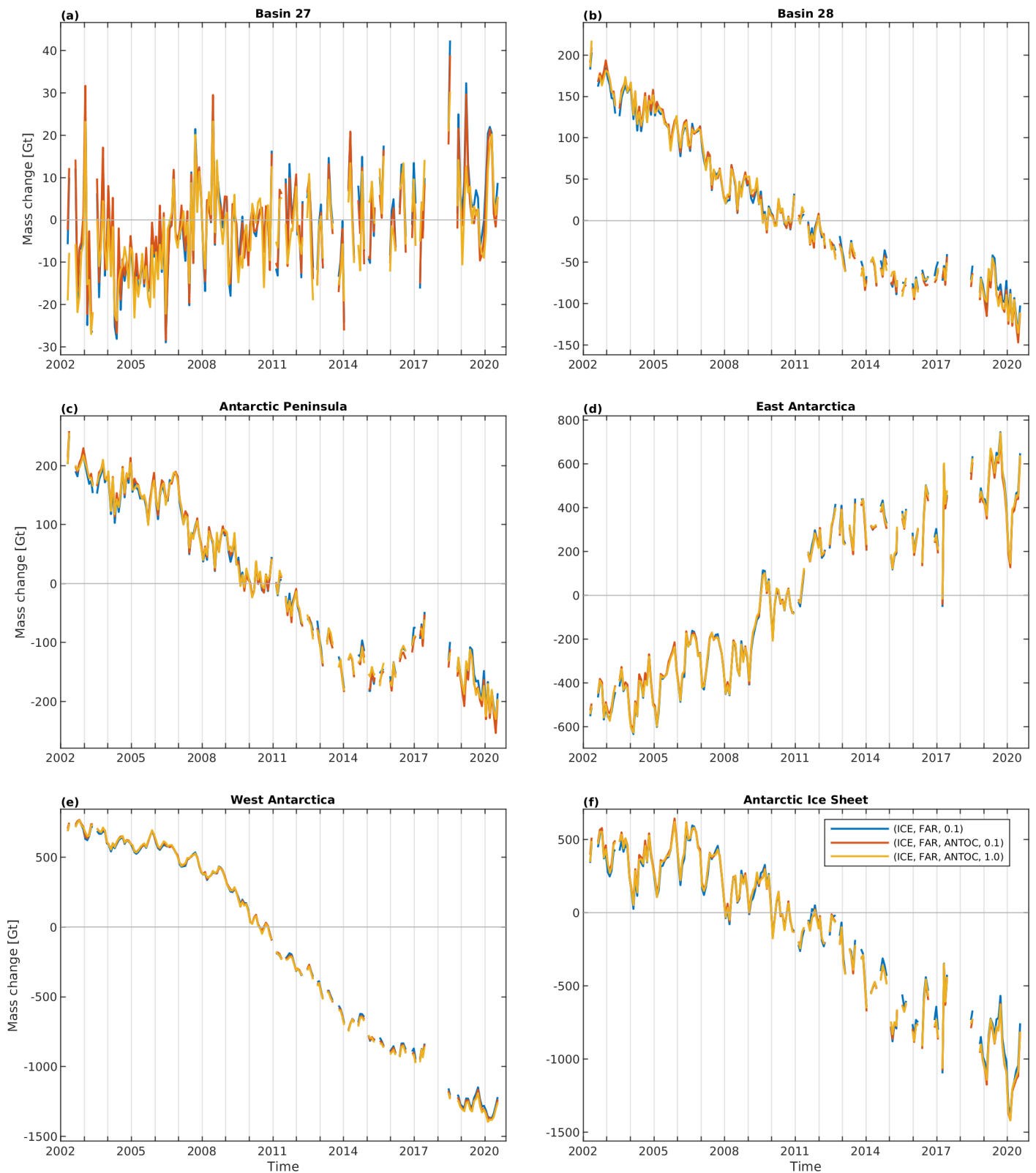


Figure S11. (a)–(f) Mass change time series for Basin 27, Basin 28, the Antarctic Peninsula, East Antarctica, West Antarctica and the entire Antarctic Ice Sheet derived using different realisations of tailored sensitivity kernels.

3. Signal Leakage

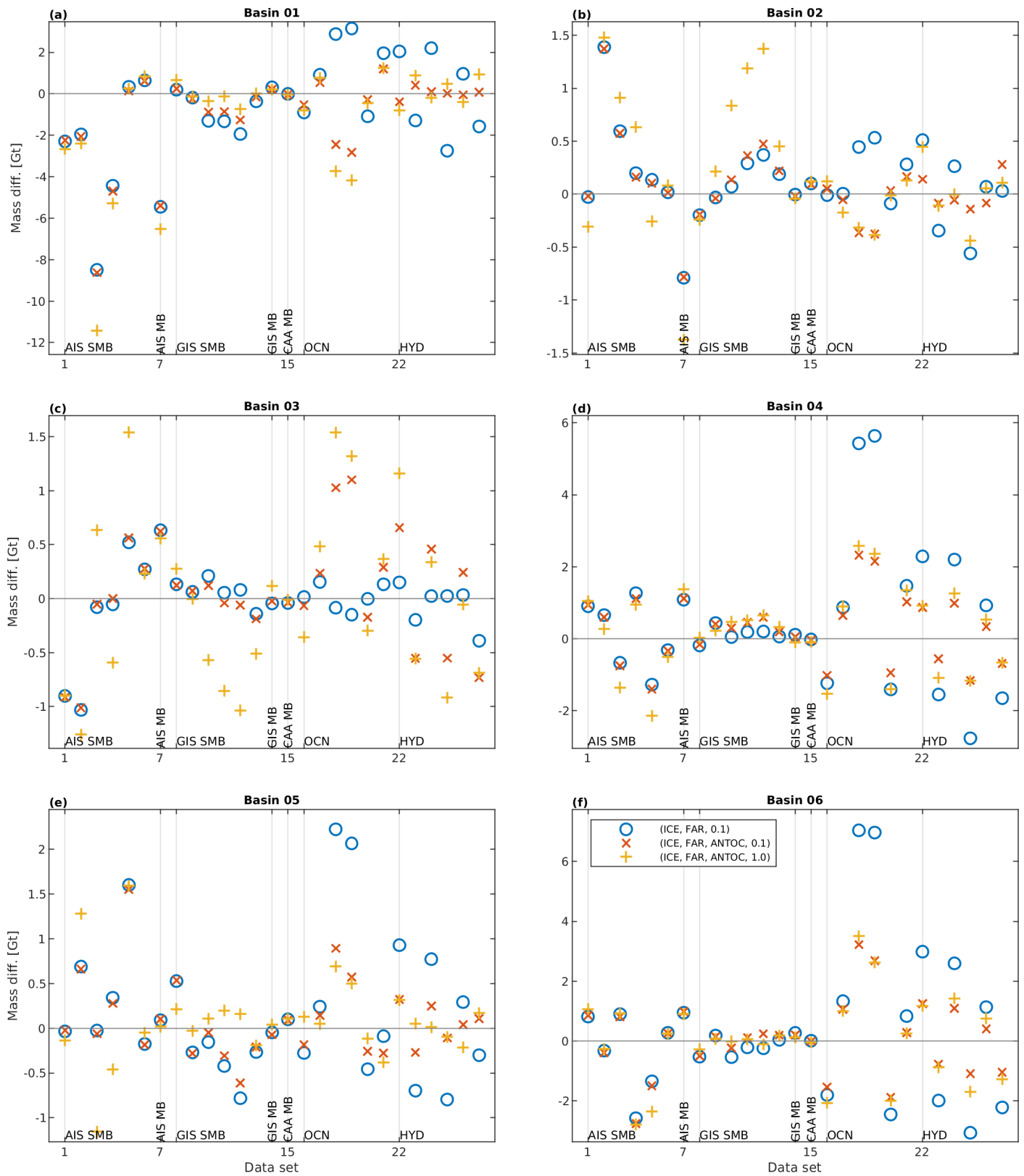


Figure S12. (a)–(f) Differences between mass change estimates derived from synthetic data sets and their corresponding true mass changes for Basin 01 – Basin 06 derived using different realisations of tailored sensitivity kernels.

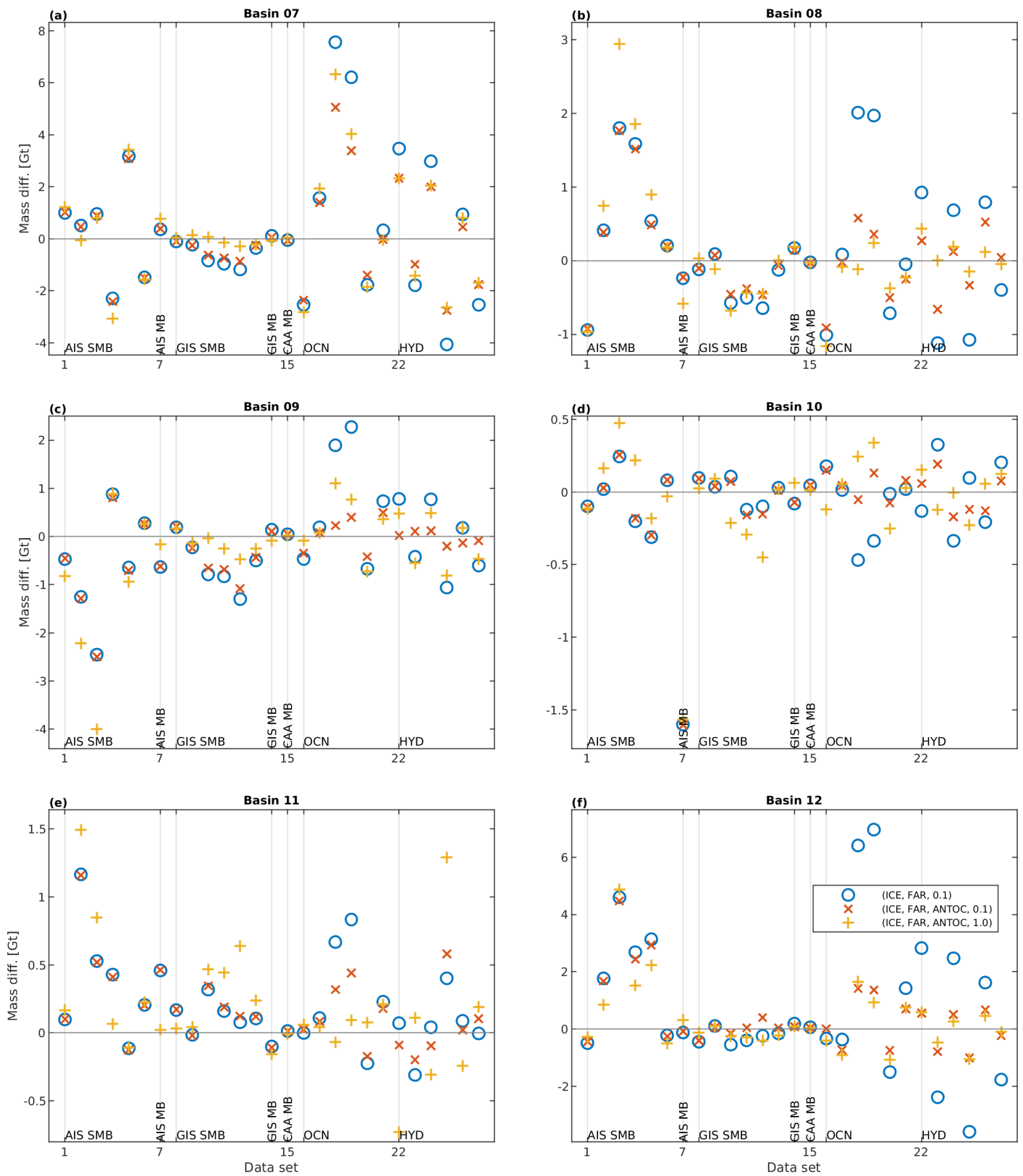


Figure S13. (a)–(f) Differences between mass change estimates derived from synthetic data sets and their corresponding true mass changes for Basin 07 – Basin 12 derived using different realisations of tailored sensitivity kernels.

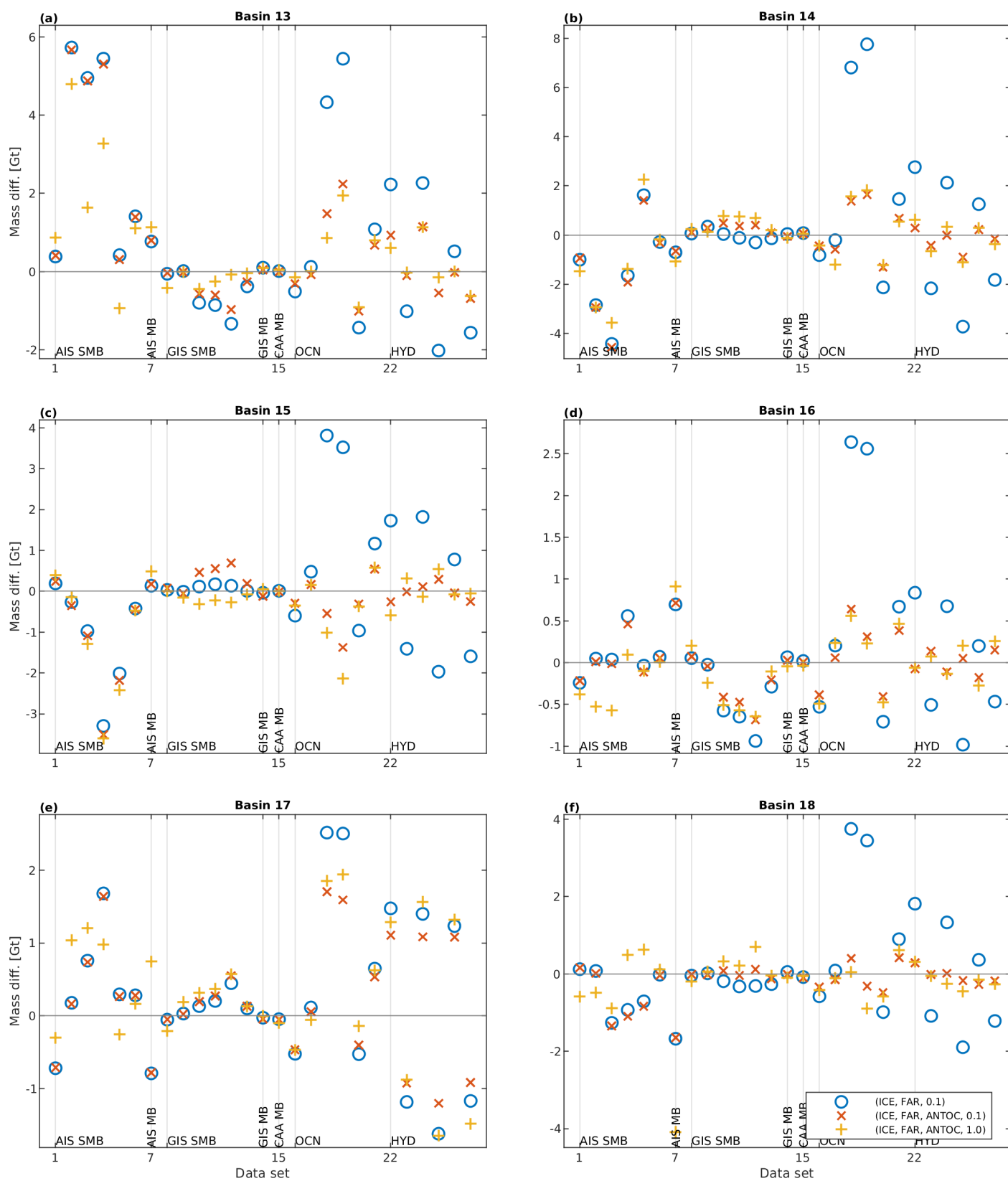


Figure S14. (a)–(f) Differences between mass change estimates derived from synthetic data sets and their corresponding true mass changes for Basin 13 – Basin 18 derived using different realisations of tailored sensitivity kernels.

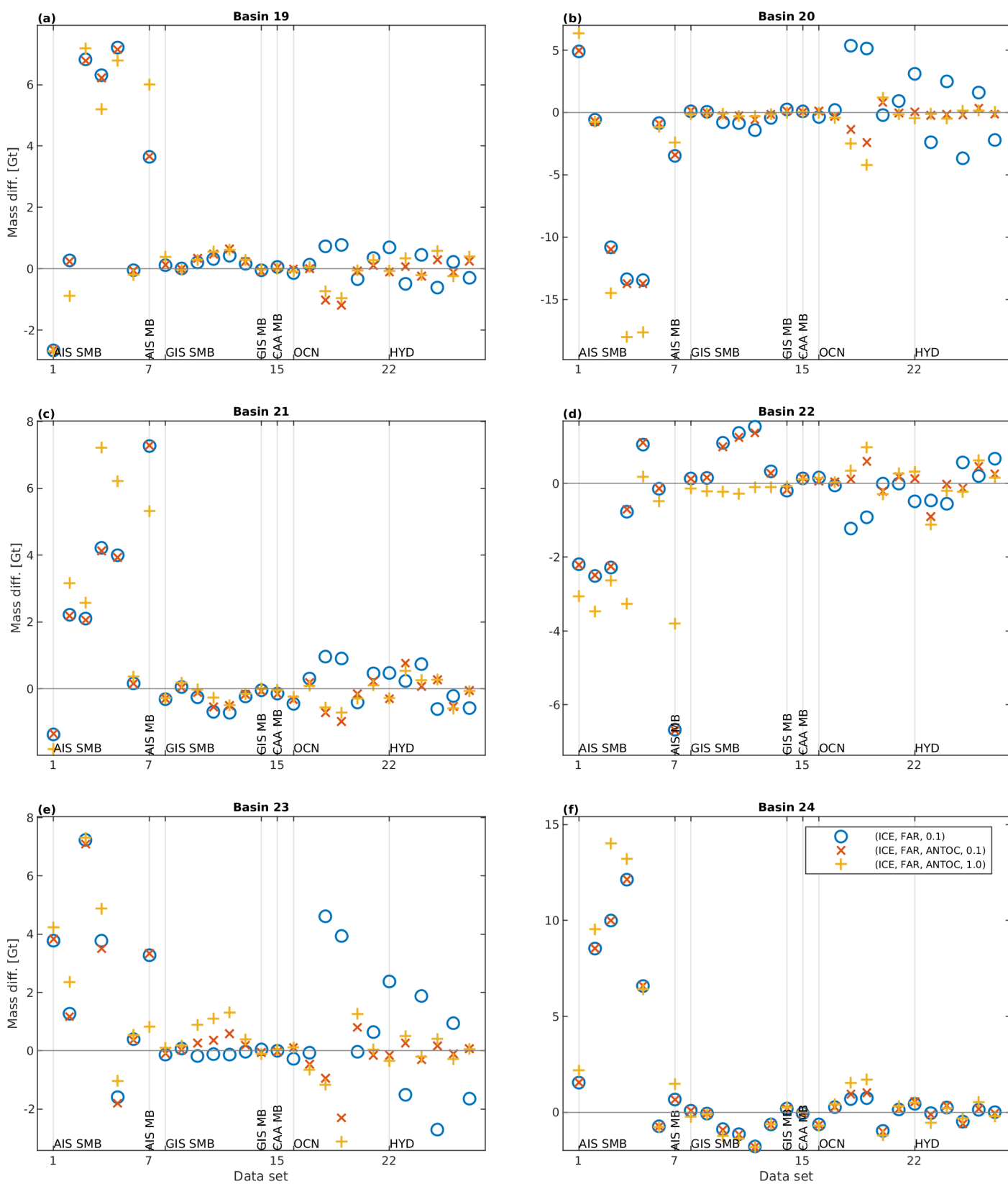


Figure S15. (a)–(f) Differences between mass change estimates derived from synthetic data sets and their corresponding true mass changes for Basin 19 – Basin 24 derived using different realisations of tailored sensitivity kernels.

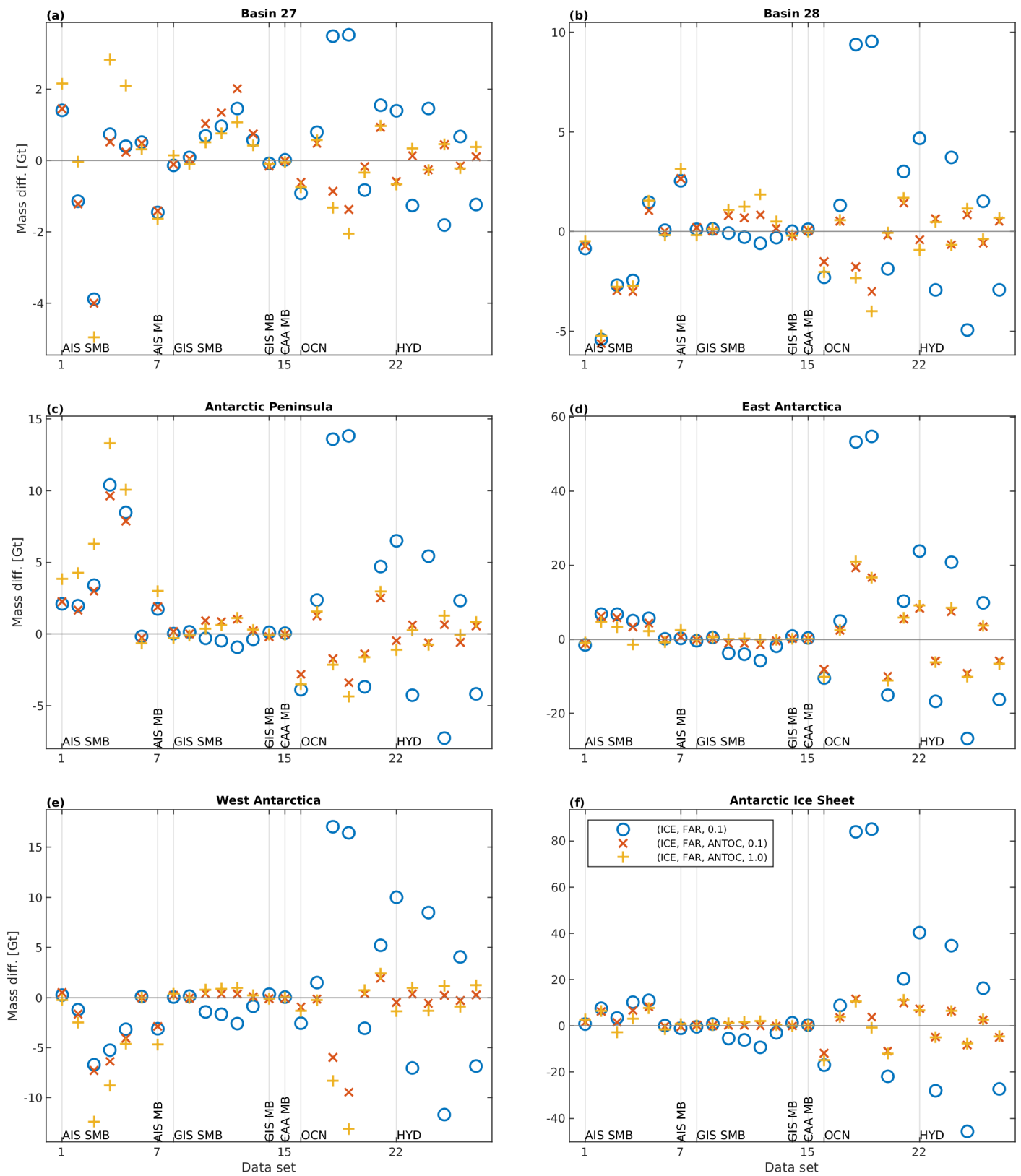


Figure S16. (a)–(f) Differences between mass change estimates derived from synthetic data sets and their corresponding true mass changes for Basin 27, Basin 28, the Antarctic Peninsula, East Antarctica, West Antarctica and the entire Antarctic Ice Sheet derived using different realisations of tailored sensitivity kernels.

4. Mass Balance Estimates

Table S1. Ice mass balance and noise level derived from the final basin products of variant (ICE,FAR,ANTOC,1.0). The mass balance is equivalent to the linear trend derived by fitting the standard model to the mass change time series from 2002-04 through 2020-07. Uncertainties account for formal errors from the least squares adjustment, uncertainties of the glacial isostatic adjustment (GIA) model correction, leakage errors, uncertainties of the degree $l = 1$ addition and the C_{20} replacement. The scaled rms of the noise time series (NRMS) is used as a measure of the noise level. The last column gives the trend of the applied GIA correction.

Region	Mass balance [Gt a ⁻¹]	Uncertainty components [Gt a ⁻¹]					NRMS [Gt]	GIA corr. [Gt a ⁻¹]
		Formal	GIA	Leakage	$l = 1$	C_{20}		
AIS01	6.2±05.7	±0.4	±3.8	±4.1	±0.8	±0.7	14.6	10.4
AIS02	3.1±04.5	±0.2	±4.0	±0.2	±1.4	±1.3	9.6	2.1
AIS03	15.1±14.1	±0.3	±13.6	±0.2	±2.8	±2.5	14.1	0.9
AIS04	9.7±02.4	±0.2	±2.2	±0.1	±0.5	±0.7	8.1	0.9
AIS05	7.6±00.9	±0.2	±0.8	±0.2	±0.3	±0.3	9.9	0.1
AIS06	17.0±02.4	±0.4	±1.8	±0.1	±1.1	±1.0	11.8	1.3
AIS07	16.9±03.8	±0.4	±3.5	±0.2	±1.0	±0.8	17.5	2.9
AIS08	6.2±01.1	±0.2	±1.1	±0.0	±0.3	±0.2	10.0	1.1
AIS09	0.8±01.4	±0.1	±1.3	±0.1	±0.3	±0.2	6.0	1.3
AIS10	2.7±06.2	±0.2	±5.8	±0.2	±1.6	±1.3	9.1	1.2
AIS11	−0.6±02.2	±0.1	±2.1	±0.2	±0.5	±0.3	6.4	1.2
AIS12	−1.0±04.1	±0.3	±3.7	±0.2	±1.3	±1.0	14.1	2.6
AIS13	−18.0±02.9	±0.4	±1.5	±0.2	±2.0	±1.5	16.4	2.2
AIS14	−3.2±03.5	±0.4	±3.1	±0.1	±1.3	±1.0	14.0	3.2
AIS15	−2.3±00.7	±0.2	±0.5	±0.1	±0.2	±0.4	9.4	0.3
AIS16	1.5±01.0	±0.1	±0.6	±0.2	±0.5	±0.6	5.6	0.1
AIS17	9.2±06.9	±0.3	±5.3	±0.2	±3.4	±2.8	17.7	0.5
AIS18	15.8±03.9	±0.1	±3.8	±0.5	±0.5	±0.5	6.6	3.6
AIS19	1.2±03.0	±0.1	±2.4	±1.6	±0.6	±0.6	5.5	3.7
AIS20	−37.3±05.8	±0.4	±1.3	±5.7	±0.3	±0.3	7.4	1.7
AIS21	−56.2±09.0	±0.3	±1.6	±8.8	±0.4	±0.4	9.6	1.8
AIS22	−51.1±10.9	±0.4	±1.0	±10.8	±0.4	±0.6	8.6	2.9
AIS23	−10.0±05.0	±0.2	±2.2	±4.5	±0.1	±0.5	5.6	1.3
AIS24	−9.0±04.8	±0.3	±1.7	±4.5	±0.3	±0.2	8.4	2.3
AIS27	0.9±03.5	±0.1	±1.7	±3.0	±0.0	±0.2	8.2	1.0
AIS28	−16.3±05.9	±0.2	±2.0	±5.5	±0.0	±0.3	12.0	0.8
AP	−24.4±07.0	±0.5	±2.7	±6.4	±0.3	±0.4	18.4	4.2
EAIS	64.8±39.1	±1.5	±31.0	±0.4	±18.5	±15.0	66.4	21.9
WAIS	−131.3±15.0	±1.5	±13.6	±4.5	±3.1	±2.7	27.0	25.4
AIS	−90.9±43.5	±1.8	±32.6	±5.5	±21.8	±17.9	84.4	51.5

Table S2. Ice mass balances derived from the final basin products of variant (ICE,FAR,ANTOC,1.0), mass changes based on altimetry-observed surface elevation changes (SEC) [1] and mass changes inferred from the input-output method (IOM) [2]. The mass balance is equivalent to the linear trend derived by fitting the standard model to the corresponding mass change time series from 2002–04 through 2016–08. Uncertainties for SEC are adopted from the original mass balance estimates for the period 1992–2017 [1] and those for IOM from the original estimates for the period 2009–2017 [3]. For regions with names given in bold, GRACE/GRACE-FO and SEC mass balance estimates agree within the uncertainties.

Region	GRACE/GRACE-FO [Gt a ⁻¹]	SEC [Gt a ⁻¹]	IOM [Gt a ⁻¹]
AIS01	5.1±05.7	5.1±02.1	
AIS02	2.8±04.5	1.8±06.2	
AIS03	16.7±14.1	6.8±00.6	
AIS04	11.0±02.4	3.8±00.6	
AIS05	7.1±00.9	3.6±00.6	
AIS06	17.5±02.4	6.9±00.8	
AIS07	16.9±03.8	7.7±00.9	
AIS08	6.7±01.1	3.4±00.5	
AIS09	1.3±01.4	1.1±00.5	
AIS10	3.8±06.2	−0.2±00.8	
AIS11	−0.4±02.2	−0.7±00.4	
AIS12	4.9±04.1	−2.3±01.3	
AIS13	−12.4±02.9	−15.2±02.0	
AIS14	−7.3±03.5	−4.9±01.0	
AIS15	−3.7±00.7	−2.6±00.8	
AIS16	1.2±01.0	0.7±00.3	
AIS17	6.7±06.9	5.1±00.8	
AIS18	15.0±03.9	11.4±01.5	
AIS19	0.9±03.0	0.1±00.8	
AIS20	−36.5±05.8	−25.6±04.0	
AIS21	−54.9±09.0	−59.6±07.2	
AIS22	−50.1±10.9	−42.2±06.2	
AIS23	−9.7±05.0	−6.2±02.1	
AIS24	−10.2±04.8	−4.8±01.5	
EAIS	72.9±39.1	14.3±05.5	
WAIS	−130.2±15.0	−116.8±12.1	
AIS	−86.2±43.5		−153.8±27
DML	48.2±04.7	21.6±01.4	28.5±13 ^a
ASS	−105.0±14.1	−101.8±09.5	−121.2±8 ^b

^a Uncertainty for entire EAIS provided in [\[3\]](#)

^b Uncertainty for entire WAIS provided in [\[3\]](#)

5. Gridded Products

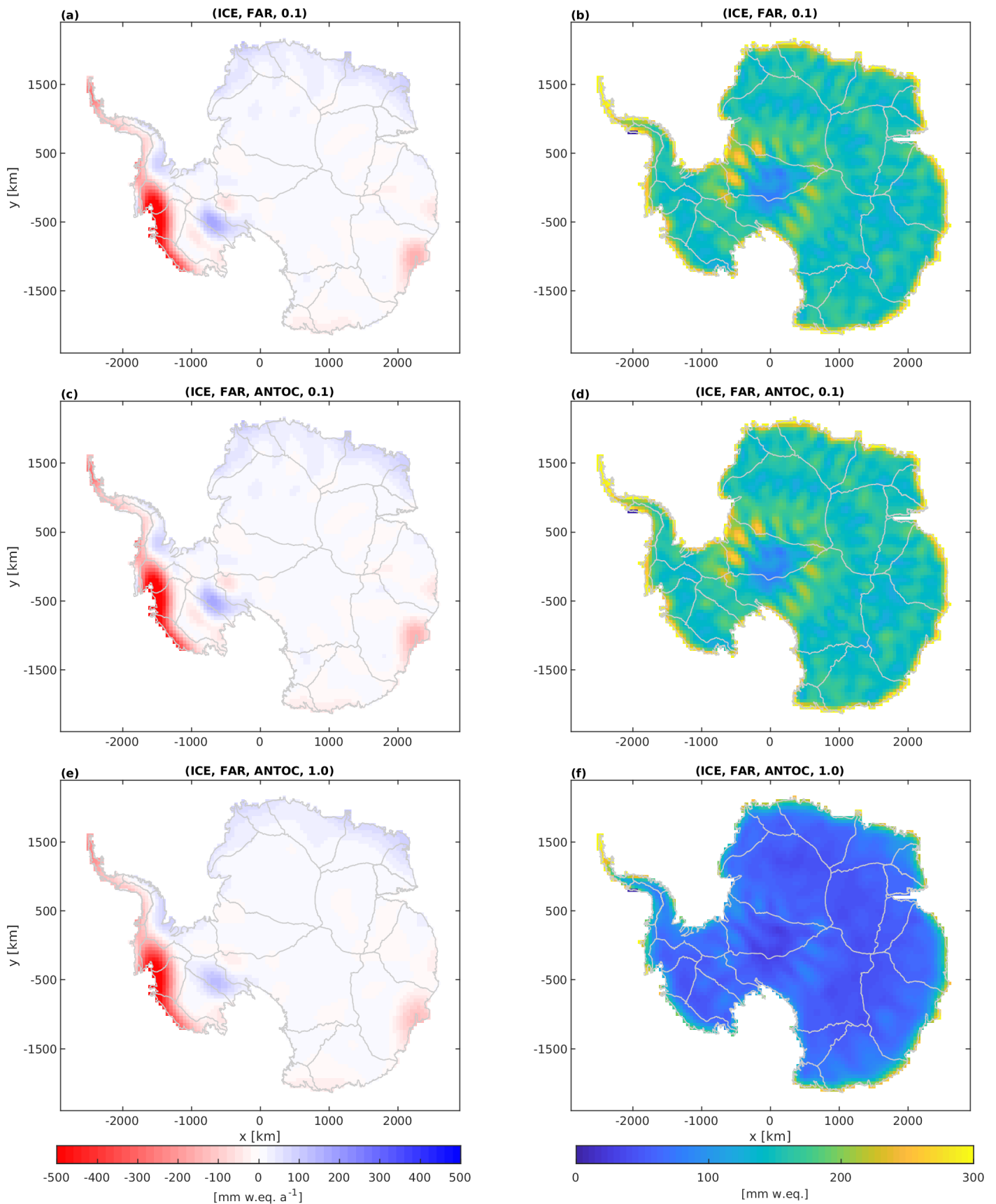


Figure S17. (a),(c),(e) Linear trend derived from the gridded mass change product using a the standard model. (b),(d),(f) Noise level of each grid cell, assessed as described in Section 2.5.2 (main text). Both quantities are based on different variants of tailored sensitivity kernels as indicated by the title of the panels.

References

1. Shepherd, A.; Gilbert, L.; Muir, A.; Konrad, H.; McMillan, M.; Slater, T.; Briggs, K.; Sundal, A.; Hogg, A.; Engdahl, M. Trends in Antarctic Ice Sheet Elevation and Mass. *Geophys. Res. Lett.* **2019**. doi:10.1029/2019GL082182.
2. Velicogna, I.; Mohajerani, Y.; A, G.; Landerer, F.; Mouginot, J.; Noel, B.; Rignot, E.; Sutterley, T.; van den Broeke, M.; van Wessem, J.; Wiese, D. Continuity of ice sheet mass loss in Greenland and Antarctica from the GRACE and GRACE Follow-On missions. *Geophys. Res. Lett.* **2020**, *47*. e2020GL087291 2020GL087291, doi:10.1029/2020GL087291.
3. Rignot, E.; Mouginot, J.; Scheuchl, B.; van den Broeke, M.; Van Wessem, J.; Morlighem, M. Four decades of Antarctic Ice Sheet mass balance from 1979–2017. *Proc. Natl. Acad. Sci. USA* **2019**, *116*, 1095–1103. doi:10.1073/pnas.1812883116.